

# Thermal Computations in a Semiconductor Die Using Surface Elements and Infinite Images

K. J. NEGUS and M. M. YOVANOVICH

Microelectronics Heat Transfer Laboratory  
University of Waterloo  
Waterloo, Ontario, Canada N2L 3G1

## ABSTRACT

A thermal analysis procedure for a semiconductor die has been developed by utilizing fundamental solutions obtained with surface element methods and arrays of images to satisfy the required boundary conditions. Non-linear thermal conductivity effects are accounted for exactly through an integral transformation. A complex example problem shows the ability of the method to solve real semiconductor problems with relatively little computational effort. The example problem also indicates that silicon may be thermally more desirable than gallium arsenide for very high power applications.

## INTRODUCTION

The importance of thermal management in modern microelectronic equipment has become increasingly recognized in recent years. In some systems which employ relatively few high performance components with substantial heat dissipation, excellent external cooling systems have been designed to minimize thermal resistance. In these systems the dies are often attached to beryllia or copper-tungsten packages which can be contacted to copper bus bars that are connected to large external cooling systems. Thus, in many aerospace, telecommunication, and high-power switching applications the total thermal resistance from the semiconductor die to ambient can be fairly small. In these applications though the thermal resistance within a silicon or gallium arsenide die now becomes the limiting factor to achieving lower overall thermal resistance. In addition to representing a significant thermal resistance, non-uniform heat conduction within the die can also lead to substantially different temperatures at different active circuits which can create a variety of electrical performance problems.

Analysis of heat conduction within a semiconductor die is complicated by the three-dimensional nature of the problem and the temperature sensitivity of the thermal conductivity of silicon and gallium arsenide. For some small-scale systems numerical techniques such as the finite element method or the finite volume method can be used to predict the temperature distribution. However, the complexity of many modern large-scale discrete or integrated devices restricts numerical solutions to only "characteristic" geometries because of the excessive computational requirements associated with the full problem.

K. J. Negus is a Graduate Research Assistant.  
M. M. Yovanovich is a Professor, Member ASME.

In this work an alternative method is developed to evaluate even large-scale systems with relatively little computational requirements (i.e. on a microcomputer). The method combines a variety of exact and approximate analytical techniques developed in recent years and takes advantage of physical assumptions commonly used for thermal characterization of a semiconductor die.

### THEORETICAL BACKGROUND

An idealized system for heat conduction for high-power microelectronic components is shown in Fig. 1 where a semiconductor die is attached to the base of a package which is in intimate contact with a large heat sink (often copper). The goal of this work is to analyse conduction within the die specifically although the resultant procedures may be applicable to a variety of thermal problems in microelectronics and aerospace. Heat conduction within the die is governed by the partial differential equation

$$\nabla \cdot (k(T)\nabla T) + \dot{q} = \rho c_p(T) \frac{\partial T}{\partial t} \quad (1)$$

where the significant temperature sensitivity of the thermal properties for silicon and gallium arsenide is noted by  $k(T)$  and  $c_p(T)$ . The internal heat generation  $\dot{q}$  is an extremely complex function of space and time and is found in theory by solving for the electrical behaviour of the entire system simultaneously with the thermal analysis. In practise though it is convenient to approximate  $\dot{q}$  by a heat flux applied at specific regions to the top of the semiconductor die in Fig. 2. This approximation is reasonable since most heat generation in a semiconductor die typically 200  $\mu\text{m}$  thick occurs within a few  $\mu\text{m}$  of the top surface. Outside the heat flux regions the remainder of the top surface is essentially adiabatic. The base of the die is modelled as isothermal in this work to reflect that in high-power applications the die is usually attached to very conductive materials. This approximation is better for gallium arsenide which has a thermal conductivity about one-third that of silicon. By further assuming that the sides of die are adiabatic and considering steady-state operation only, the governing partial differential equations and boundary conditions for heat conduction within the die are

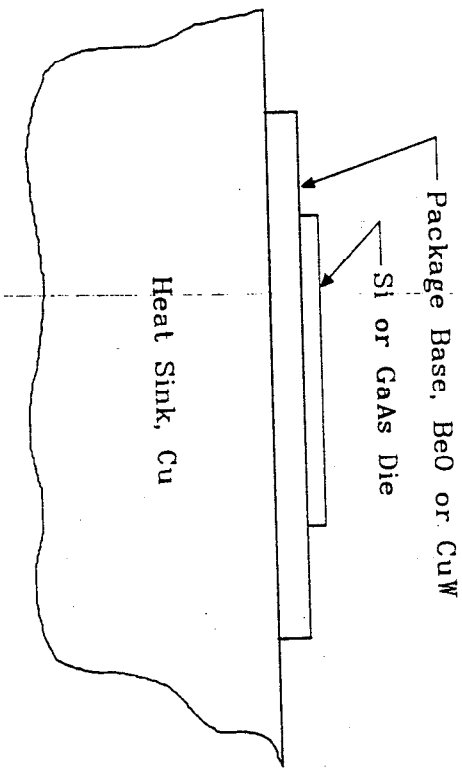


FIGURE 1. Die attachment for thermal model

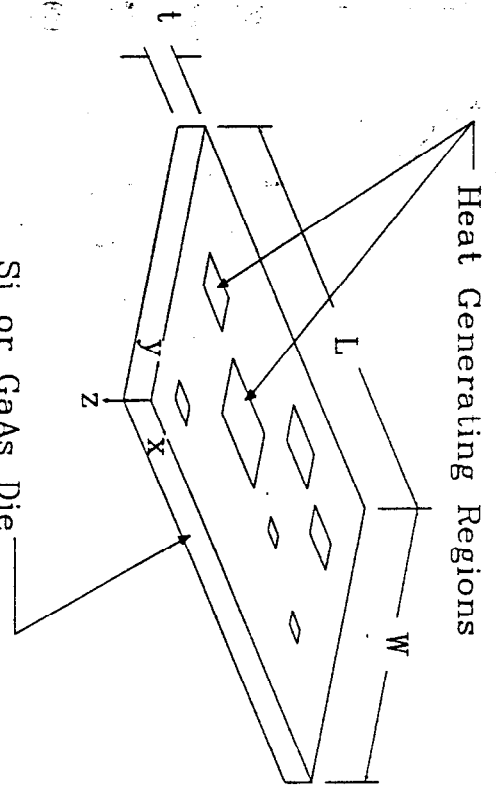


FIGURE 2. Surface heat generation regions on die

$$\nabla \cdot (k(T)\nabla T) = 0 \quad (2)$$

$$-k(T(x, y, 0)) \frac{\partial T}{\partial x}(x, y, 0) = q(x, y) \quad (3)$$

$$\frac{\partial T}{\partial z}(0, y, z_1) = \frac{\partial T}{\partial x}(L, y, z) = \frac{\partial T}{\partial y}(x, 0, z) = \frac{\partial T}{\partial y}(x, W, z) = 0 \quad (4)$$

$$T(x, y, t) = T_b \quad (5)$$

where  $q(x, y)$  is the heat flux distribution applied to the top surface of the die. The base temperature  $T_b$  is related to the total heat dissipation  $Q$  and the thermal resistance  $R_{\infty}$  from base to ambient  $T_{\infty}$  according to

$$T_b = T_{\infty} + QR_{\infty} \quad (6)$$

where

$$Q = \int_{x=0}^L \int_{y=0}^W q(x, y) dy dx \quad (7)$$

At this point one could attempt to solve Eqs. (2)-(7) with a numerical method such as finite elements or finite volumes for a given system. However, the computational problem associated with the non-linearity of the thermal conductivity can be removed entirely by applying the Kirchhoff transformation as described by Ozisik (1980). In this integral transformation, a transformed temperature  $U$  is defined as

$$U = \int_{T_{ref}}^T \frac{k(T^p)}{k(T_{ref}^p)} dT^p \quad (8)$$

where  $T_{ref}$  is some arbitrary reference temperature. In this work  $T_{ref}$  is assumed to be the ambient temperature  $T_{\infty}$ . In addition since excellent correlations of thermal conductivity versus temperature exist in the form of power laws for silicon and gallium arsenide, the thermal conductivity is assumed to be of the form

$$k(T) = k_{\infty} \left( \frac{T}{T_{\infty}} \right)^p \quad (9)$$

where  $k_{\infty}$  is the thermal conductivity of the die at ambient temperature and  $p$  is the power law exponent for the temperature range of interest.

The transformed temperature  $U$  is thus related to the actual temperature  $T$  according to the relationships

$$U = \frac{T_{\infty}}{p+1} \left[ \left( \frac{T}{T_{\infty}} \right)^{p+1} - 1 \right] \quad (10)$$

or

$$T = T_{\infty} \left[ 1 + (p+1) \frac{U}{T_{\infty}} \right]^{\frac{1}{p+1}} \quad (11)$$

where  $p \neq -1$  has been assumed. The problem can be further simplified for analysis purposes by introducing

$$\phi = U - U_b = U - \frac{T_{\infty}}{p+1} \left[ \left( \frac{T}{T_{\infty}} \right)^{p+1} - 1 \right] \quad (12)$$

Eqs. (2)-(5) now become in terms of the transformed variable  $\phi$

$$\nabla^2 \phi = 0 \quad (13)$$

$$-k_{\infty} \frac{\partial \phi}{\partial x}(x, y, 0) = q(x, y) \quad (14)$$

$$\frac{\partial \phi}{\partial x}(0, y, z) = \frac{\partial \phi}{\partial x}(L, y, z) = \frac{\partial \phi}{\partial y}(x, 0, z) = \frac{\partial \phi}{\partial y}(x, W, z) = 0 \quad (15)$$

$$\phi(x, y, l) = 0 \quad (16)$$

This linear three-dimensional problem governed by Laplace's equation can now be solved by a variety of analytical and numerical techniques. For example, Fourier's method can be used to construct an eigenfunction solution in terms of a double-infinite series. Unfortunately though, the computation associated with this exact solution can be tremendous since many thousands of terms are required especially with increasing complexity of the heat flux distribution  $q(x, y)$ . In practice, the heat flux can usually be visualized as a series of rectangular contact areas as shown in Fig. 2. For each contact the heat flux is usually fairly uniform and certainly can be approximated as

uniform for lack of better information. This assumption combined with the linearity of Laplace's equation allows an analysis of this problem by combining the Surface Element Method (Yovanovich et al., 1983) and the Method of Infinite Images (Negus et al., 1985).

To construct the solution to Eqs. (13)-(16) with this approach, the temperature rise due to a single planar contact in an infinite space (or full space) must be evaluated. In Fig. 3 an arbitrary planar contact area of infinitesimal thickness and heat dissipation rate  $2q_0$  per unit area is located in a plane a distance  $h$  directly below some point  $P$ . The temperature rise  $\phi$  at  $P$  can be written as (Yovanovich et al., 1983)

$$\phi = \frac{2q_0}{4\pi k_{\infty}} \int_A \frac{dA}{\rho} \quad (17)$$

In terms of a local polar coordinate system with origin at the centroid this becomes

$$\phi = \frac{q_0}{2\pi k_{\infty} R} \int_A \left[ 1 + \left( \frac{r}{R} \right)^2 - \frac{2rR_0}{R^2} \cos \theta \right]^{-1/2} dA \quad (18)$$

Expansion by the binomial theorem (assuming  $P$  is located far from the contact) gives

$$\phi = \frac{q_0}{2\pi k_{\infty} R} \left[ \int_A dA + \frac{R_0^2}{R^2} \int_A r \cos \theta dA - \frac{1}{2R^2} \int_A r^2 dA + \frac{3R_0^2}{2R^4} \int_A r^2 \cos^2 \theta dA + \dots \right] \quad (19)$$

The first integral in Eq. (19) is simply the area of the contact  $A$ , and the second integral is zero identically by the definition of the centroid. Thus Eq. (19) can be written as

$$\phi = \frac{q_0}{2\pi k_{\infty}} \left[ \frac{A}{R} + \frac{3 \cos^2 \omega - 1}{2R^3} \int_A r^2 dA - \frac{3 \cos^2 \omega}{2R^3} \int_A r^2 \sin^2 \theta dA + \dots \right] \quad (20)$$

The remaining two integrals shown in Eq. (20) are recognizable from basic calculus as

$$I_0 = \int_A r^2 dA \quad (21)$$

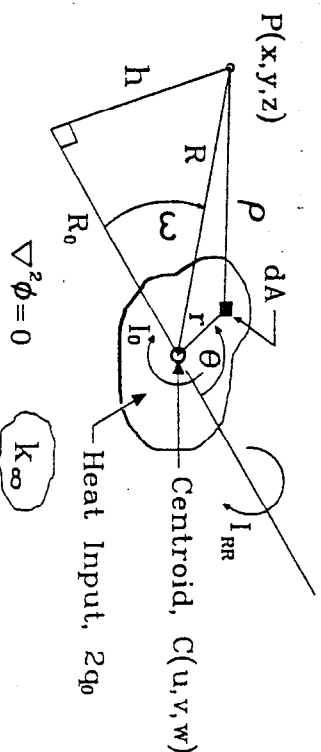


FIGURE 3. Temperature rise at point exterior to arbitrary planar contact

$$I_{RR} = \int_A r^2 \sin^2 \theta dA \quad (22)$$

where  $I_0$  is the polar second moment of area about the centroid of the contact and  $I_{RR}$  is the radial second moment of area about the axis formed by the projection of PC onto the plane  $z = w$ . After truncating all higher-order terms, Eq. (20) can be written as

$$\phi \approx \frac{q_0}{2\pi k_{\infty}} \left[ \frac{A}{R} + \frac{3 \cos^2 \omega (I_0 - I_{RR}) - I_0}{2R^3} \right] \quad (23)$$

where accuracy decreases rapidly for  $R/\sqrt{A} < 2$ .

For common shapes such as rectangles, simple algebraic expressions for  $I_0$  and  $I_{RR}$  are readily available as discussed in Negus et al. (1985). In this application all contacts are rectangular in shape and in the simple examples to follow only square contacts are used. With this restriction it is easy to evaluate the temperature rise at points close to the contact simply by micro-discretization into smaller square or rectangular contacts as required (increased effective  $R/\sqrt{A}$  for the smaller contacts). This is extremely simple to implement in a computer code and simple empirical formulae have been developed to ensure that errors much less than 1% are achieved. If the point  $P$  at which the temperature rise is sought lies within the rectangular planar contact, then the straightforward algebraic expressions for the exact solution developed by Yovanovich (1976) are utilized.

At this point a simple solution approach exists to determine the transformed temperature rise of any rectangular contact. With the linearity of Eq. (13) the temperature rises due to all contacts in the system can be superposed to satisfy Eqs. (13) and (14). To satisfy Eq. (15) and (16) a theoretically infinite number of identical rectangular contacts are needed.

Consider first the images required to satisfy Eq. (16). As shown in Fig. 4 it is thus desired to obtain the solution for a contact releasing heat into a domain bounded by an adiabatic plane and an isothermal plane. A single starting source denoted as number 0 in Fig. 4 and assumed to have positive heat flux applied to it satisfies the adiabatic plane criterion but not the isothermal plane. If an image with negative heat flux is assumed to be located directly below the starting source as shown by image number 1 in Fig. 4, then the superposition of both contacts gives the isothermal plane as desired. However the adiabatic plane no longer exists. Thus a second image (number 2) also of negative heat flux must be placed above the starting source as shown in Fig. 4 to restore the adiabatic plane but unfortunately also destroy the isothermal plane. This procedure of alternating images above and below the source must then be repeated to form an exact solution for  $\phi(x, y, z)$  in the solution region shown in Fig. 4 in the form of an infinite series of images. In practice the series obtained is extremely slow to converge and often requires several thousand terms to obtain error less than 1%. However, this problem can be completely avoided by applying the Euler transformation to the series (Oliver, 1974) which reduces the required number of terms down to 8-10 typically. The Euler transformation is excellent from a computational viewpoint because it not only reduces the number of terms to be evaluated substantially, but also accomplishes this goal with virtually no extra multiplications (mainly subtractions).

Superposition of all contacts and required images now satisfies Eqs. (13), (14) and (16). The final boundary condition of adiabatic sides on the die (Eq. (15)) can also be satisfied with the infinite image approach. The required distribution of images is shown in plan view in Fig. 5. Note that each image of the starting source has identical heat flux applied to it and each consists of a series of infinite images in the  $x$  direction as previously described for the starting source. In practice even the first row of images shown in Fig. 5 rarely makes any significant contribution for the points of maximum temperature rise within the die due to the relative thinness of a typical semiconductor die. Thus these images, though available in the computer program associated with this work, are needed only occasionally.

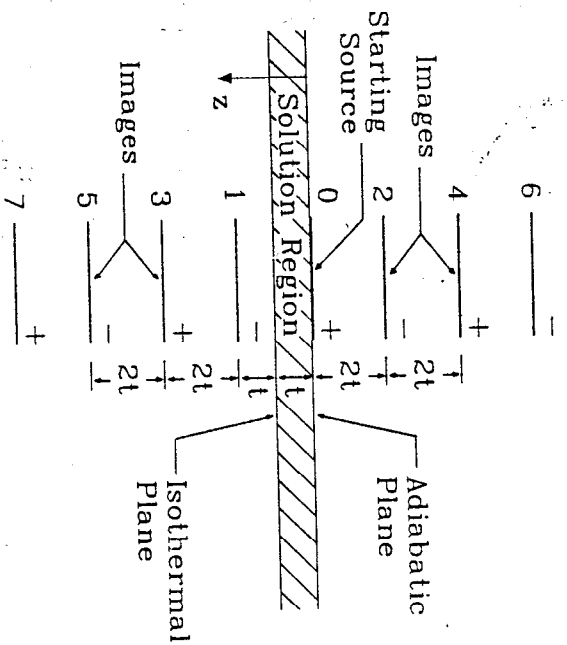


FIGURE 4. Images required above and below die

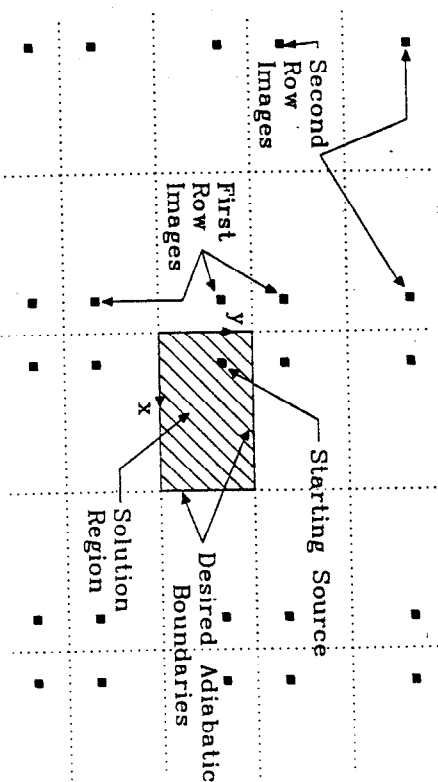


FIGURE 5. Images required along sides of die

With the images described an exact solution for the transformed temperature rise  $\phi$  throughout the die is now available since Eqs. (13)-(16) are all satisfied. This solution can be visualized conceptually as having the form

$$\phi(x, y, z) = \sum_{i=1}^N \sum_{j=1}^{\infty} \phi_{ijk}(x, y, z, u_{ijk}, v_{ijk}, w_{ijk}, a_i, q_j) \quad (24)$$

In summary,  $\phi_{ijk}(\cdot)$  represents the temperature rise contribution due to an individual source. By assuming that square contacts are used,  $\phi_{ijk}$  is then a function only of the coordinates of the desired point  $P(x, y, z)$ , the coordinates of the source or image contact  $C(u_{ijk}, v_{ijk}, w_{ijk})$ , the width  $a_i$  of the  $i$ th square contact and the heat flux  $q_j$  applied to the  $j$ th contact in the system.  $N$  represents the number of contact areas on the surface of the semiconductor die and can potentially range from one to several thousand. The first infinite summation ( $j = 1$  to  $\infty$ ) represents the images above and below the die and the practical upper bound on the sum is typically 8-10 as discussed previously. The second infinite summation ( $k = 1$  to  $\infty$ ) refers to the images shown in Fig. 5 which are usually either not required at all or only contribute significantly from a few in the first row. Each evaluation of  $\phi_{ijk}$  is given by simple algebraic expressions derived either from Eq. (23) for points  $P(x, y, z)$  exterior to the contacts or from the work of Yovanovich (1976) for points within a rectangular planar contact. After the transformed temperature at any point is determined by applying Eq. (24), the real temperature rise can be readily calculated from Eqs. (10) - (12).

### EXAMPLE RESULTS

The application of the preceding methodology to an actual heat conduction problem can be demonstrated by considering the geometry shown in Fig. 6. The contact distribution of this semiconductor die has not been derived from any real application in particular but is indicative of the complexity possible in practice. Quantitative results for the temperature rise in the die shown in Fig. 6 have been computed for the dimensions shown with die thicknesses of 250  $\mu\text{m}$  and 150  $\mu\text{m}$  and die ma-

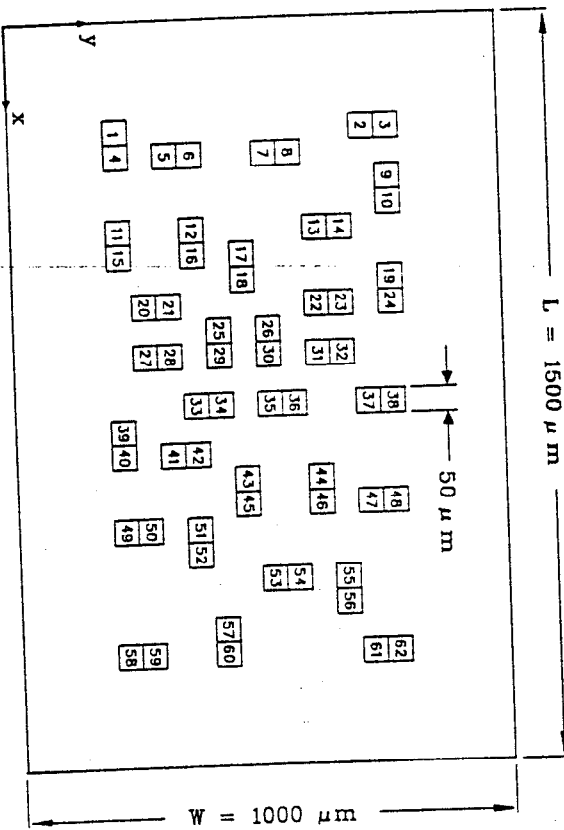


FIGURE 6. Surface contact distribution of die for example problem

terials of silicon and gallium arsenide. The thermal conductivities of silicon and gallium arsenide are assumed to be given by the power laws (Maycock, 1967)

$$k_{Si} = 2600T^{-1.33} \quad (\text{W/cmK}) \quad (25)$$

$$k_{GaAs} = 1707T^{-1.06} \quad (\text{W/cmK}) \quad (26)$$

which are valid for temperature within the normal operating range of these materials ( $300 < T < 500$  K for silicon  $300 < T < 700$  K for gallium arsenide). The die is assumed to be attached to a beryllia base 5 mm thick which is in intimate contact with a large copper heat sink as originally shown in Fig. 1. This arrangement has an estimated external resistance of  $R_{\infty} = 2(\text{K/W})$  for this die size and an ambient temperature of  $T_{\infty} = 300$  K has been assumed. The actual results of the thermal analysis for the four different cases are given in Table 1 for a total heat dissipation rate of 20 W assumed to be uniformly distributed over all the contact areas shown in Fig. 6. All

Contact Number	Centroidal Contact Temperature (K)			
	Silicon		Gallium Arsenide	
	$t=250 \mu\text{m}$	$t=150 \mu\text{m}$	$t=250 \mu\text{m}$	$t=150 \mu\text{m}$
1	400	388	566	514
2	403	390	578	521
3	401	389	571	518
4	404	391	584	525
5	409	394	606	538
6	408	392	601	531
7	407	391	597	526
8	407	391	597	527
9	408	393	603	537
10	410	393	608	537
11	410	393	611	535
12	421	400	663	565
13	419	398	651	556
14	418	398	649	558
15	413	394	622	542
16	427	404	692	583
17	427	403	691	578
18	432	406	716	594
19	414	395	628	544
20	424	402	675	573
21	431	407	709	595
22	431	407	714	595
23	429	405	700	589
24	415	398	632	546
25	412	412	756	620
26	439	439	755	618
27	424	401	676	571
28	433	408	721	601
29	441	413	765	626
30	441	413	765	625
31	435	409	732	607

TABLE 1a. Centroidal contact temperature distribution for example problem (contacts 1-31)

Contact Number	Silicon		Gallium Arsenide	
	$t=250 \mu\text{m}$	$t=150 \mu\text{m}$	$t=250 \mu\text{m}$	$t=150 \mu\text{m}$
32	429	405	701	588
33	435	409	732	605
34	437	410	743	611
35	435	408	732	601
36	431	405	714	589
37	417	398	643	550
38	410	392	611	530
39	414	395	631	544
40	414	395	631	545
41	427	404	692	583
42	430	406	707	591
43	427	402	690	576
44	421	399	660	560
45	424	401	677	571
46	420	399	656	561
47	413	395	623	544
48	406	390	592	523
49	407	391	599	528
50	414	396	629	549
51	400	385	602	567
52	416	397	639	553
53	414	396	630	547
54	415	397	633	552
55	411	395	615	543
56	408	394	603	538
57	405	391	590	526
58	395	385	545	501
59	398	387	557	509
60	401	388	571	515
61	399	388	560	513
62	396	385	548	504

TABLE 1b. Centroidal contact temperature distribution for example problem (contacts 32-62) results reported in Table 1 represent centroidal temperatures in K corresponding to the contact numbering scheme shown in Fig. 6.

These results indicate a tremendous difference in the thermal response of silicon and gallium arsenide for a high-power application. The temperature rises on the silicon die are obviously much lower than those on the gallium arsenide die of same thickness. This can be attributed first to the higher thermal conductivity of silicon ( $k_{Si} \sim 2.5k_{GaAs}$  for same  $T$ ) and second to the non-linear conductivity effect of decreasing thermal conductivity with increasing temperature. As a result of these effects the peak internal thermal resistance for the die alone (based on maximum die temperature rise divided by total heat dissipation rate) is approximately 21 ( $K/W$ ) for gallium arsenide and only 5 ( $K/W$ ) for silicon when a 250  $\mu\text{m}$  thick die is used. When a thinner die of 150  $\mu\text{m}$  is considered, this resistance is reduced substantially to 14 ( $K/W$ ) and 3.7 ( $K/W$ ) respectively. Thicker dies are generally favoured for ease of manufacture but these results clearly show that they are thermally undesirable for high-power applications.

Finally, all computations associated with Table 1 were performed in BASiC on an IBM-PC with a total execution time of approximately one hour. With the new CAE workstations under development, execution times 2 orders of magnitude lower than that of the IBM-PC are possible which would make thermal analysis of this type very attractive as a CAD tool for semiconductor design engineers.

#### CONCLUSIONS

An efficient methodology to compute temperatures within a semiconductor die has been developed. This method takes advantage of the surface heating nature of the problem and the usual rectangular shape of the heat generation zones. The approach is based on fundamental solutions to Laplace's equation obtained by surface element methods. The boundary conditions describing the finite geometry of the die are then satisfied by a theoretically infinite series of images. The extreme temperature dependency of common semiconductors is also accounted for exactly through an integral transformation.

The utility of the method has been illustrated by examining an example problem with a complex surface contact distribution. The results obtained show superior performance for silicon over gallium arsenide for high power applications even with the higher temperature capabilities of gallium arsenide devices. Therefore the most important application for this method at this time may be in the layout of gallium arsenide circuits since the internal resistance is extremely significant and the assumption of an isothermal base for the die is more valid for a lower thermal conductivity semiconductor.

The computational efficiency of this method makes it ideal as a CAD tool for designers involved in the circuit layout of semiconductor dies. In addition, thermal analysis can be coupled with electrical CAD tools as demonstrated by Negus et al. (1987) to provide capability for complete thermal-electrical analysis of semiconductor devices.

#### ACKNOWLEDGEMENTS

The authors acknowledge the financial support of this work by the Natural Sciences and Engineering Research Council of Canada under operating grant A7455 for Dr. Yovanovich and from a Postgraduate Scholarship for Mr. Negus.

#### NOMENCLATURE

- $a_i$  — width of  $i^{\text{th}}$  square contact
- $A$  — area of arbitrary planar contact
- $I_p$  — polar second moment of area of arbitrary planar contact
- $I_{RR}$  — radial second moment of area of arbitrary planar contact
- $k$  — thermal conductivity
- $k_{ao}$  — thermal conductivity at ambient temperature
- $L$  — length of die
- $p$  — power law parameter for thermal conductivity correlation

- $q$  — heat flux at surface
  - $q_i$  — uniform heat flux applied to  $i^{\text{th}}$  square contact
  - $Q$  — total heat dissipation rate of die
  - $R$  — distance to centroid of arbitrary planar contact
  - $R_{\text{th}}$  — thermal resistance from base of die to ambient
  - $t$  — thickness of die
  - $T$  — temperature (always in K)
  - $T_b$  — base temperature of die
  - $T_{\infty}$  — ambient temperature
  - $U$  — transformed temperature
  - $w$  — width of die
  - $x, y, z$  — Cartesian coordinate system
- Greek Symbols
- $\rho$  — distance to elemental area on arbitrary contact
  - $\phi$  — transformed temperature for homogeneous problem
  - $\omega$  — projection angle from arbitrary planar contact to point of temperature calculation

## REFERENCES

- Maycock, P.D. 1967, "Thermal Conductivity of Silicon, Germanium, III-V Compounds and III-V Alloys", *Solid State Electron*, Vol. 10, pp. 161-168.
- Negus, K.J., Yovanovich, M.M., and DeVal, J.W., "Development of Thermal Constriction Resistance for Anisotropic Rough Surfaces by the Method of Infinite Images", ASME Paper No. 85-HT-17, 23rd ASME-AICHE National Heat Transfer Conference, Denver, CO.
- Negus, K.J., Yovanovich, M.M., and Roulaon, D.J., 1987, "An Introduction to Thermal-Electrical Coupling in Bipolar Transistors", accepted at the Second ASME-JSME Thermal Engineering Joint Conference, Honolulu, Hawaii.
- Olver, F.W.J., 1974, *Asymptotics and Special Functions*, Academic Press, New York.
- Ozisk, M.N., 1980, *Heat Conduction*, Wiley-Interscience, New York.
- Yovanovich, M.M., 1976, "Thermal Constriction Resistance of Contacts on a Half-Space: Integral Formulation", *AIAA Progress in Astronautics and Aeronautics: Radiative Transfer and Thermal Control*, Vol. 44, edited by A.M. Smith, New York, pp.397-418.
- Yovanovich, M.M., Thompson, J.C., and Negus, K.J., 1983, "Thermal Resistance of Arbitrarily Shaped Contacts", Third International Conference on Numerical Methods in Thermal Problems, Seattle, WA.

## Three-Dimensional Natural Convection Cooling of an Array of Heated Protrusions in an Enclosure Filled with a Dielectric Fluid

K. V. LIU and K. T. YANG

Department of Aerospace and Mechanical Engineering  
University of Notre Dame  
Notre Dame, Indiana 46556, USA

M. D. KELLEHER  
Department of Mechanical Engineering  
Naval Postgraduate School  
Monterey, California 93943, USA

### ABSTRACT

A numerical finite-difference study has been carried out for laminar natural convection cooling of an array of chips mounted on a vertical wall of a three-dimensional rectangular enclosure filled with Fluorinert FC 75, a dielectric liquid. All enclosure vertical surfaces are insulated except those locations occupied by the chips, while the top and bottom horizontal surfaces are maintained constant at the room temperature. The enclosure is taken to be 144 mm long and 120 mm high, and the width is allowed to vary between 9 mm and 30 mm. Nine protruding chips, each 24 mm in height, 8 mm in width, and 6 mm in protrusion thickness and dissipating 0.4 W are uniformly placed on a vertical wall. The finite-difference calculations are based on primitive variable, micro-control volume, staggered cell, and non-uniform grid algorithm with implementation of the QUICK scheme to minimize false diffusion. Full property variation effects are accounted for. Results are given in terms of chip surface temperatures, flow patterns, and isotherms, and are then used to assess the physical mechanisms responsible for the effects of varying enclosure width.

### INTRODUCTION

Immersion cooling of electronic packages with dielectric fluids by means of natural convection has received much attention recently because of its potentially high-dissipation capabilities, together with such added advantages as no noise and high reliability. In many applications, the electronic devices being cooled are mounted on walls and encased in closed enclosures filled with dielectric liquids, and the cooling is essentially by natural convection. Much more basic data than currently exists are needed as inputs to the design of such cooling systems for optimum thermal performance. The primary reason for this is that several physical features unique to the natural-convection immersion cooling problem have not been addressed in the vast literature on the phenomena of buoyancy-driven enclosure flow and heat transfer according to the recent reviews by Hoogendoorn (1986), deVahl Davis (1986), and Yang (1986), nor adequately by recent research in the field of electronic cooling (Bar-Cohen 1986). These unique features include mounting microelectronic chips on vertical walls which often protrude into the enclosure in the form of regular arrays.

K. V. Liu is currently at the Argonne National Laboratory, Argonne, IL 60439.